Science AAAS

Title: Direct observation of closed magnetic flux trapped in the high latitude magnetosphere‡

Authors: R. C. Fear[1†*], S. E. Milan[1,2], R. Maggiolo[3], A. N. Fazakerley[4], I. Dandouras[5,6], S. B. Mende[7]

Affiliations:

[1]Department of Physics & Astronomy, University of Leicester, Leicester, UK.

[2]Birkeland Centre for Space Sciences, University of Bergen, Norway

[3]Belgian Institute for Space Aeronomy, Brussels, Belgium.

[4]Mullard Space Science Laboratory, University College London, Dorking, UK.

[5]University of Toulouse, UPS-OMP, UMR 5277, IRAP , Toulouse, France.

[6]CNRS, IRAP, Toulouse, France.

[7]Space Sciences Laboratory, University of California Berkeley, Berkeley, California, USA.

†Now at: School of Physics & Astronomy, University of Southampton, Southampton, UK.

*Correspondence to: R.C.Fear@soton.ac.uk.

Abstract: The structure of Earth's magnetosphere is poorly understood when the interplanetary magnetic field is northward. Under this condition, uncharacteristically energetic plasma is observed in the magnetotail lobes, which is not expected in the textbook model of the magnetosphere. Using satellite observations, we show that these lobe plasma signatures occur on high latitude magnetic field lines that have been closed by the fundamental plasma process of magnetic reconnection. Previous authors have suggested that closed flux can become 'trapped' in the lobe. Their hypothesis holds that this plasma trapping process explains another poorly understood phenomenon: the presence of auroras at extremely high latitudes, called transpolar arcs. Observations of the aurora at the same time as the lobe plasma signatures reveal the presence of a transpolar arc. The excellent correspondence between the transpolar arc and the 'trapped' closed flux at high altitudes provides very strong evidence of the trapping mechanism as the cause of transpolar arcs.

One Sentence Summary: Plasma observed in the magnetotail lobes is due to 'trapped' closed magnetic flux, and reveals the process behind the formation of transpolar arcs.

Main Text: The night side of the terrestrial magnetosphere forms a structured magnetotail, consisting of a plasma sheet at low latitudes that is sandwiched between two regions called the magnetotail lobes (Fig 1.). The lobes consist of the regions in which the terrestrial magnetic field lines are directly connected to the interplanetary magnetic field (IMF), which is referred to as being topologically 'open' (indicated by the dashed gray lines in Fig. 1). Magnetic field lines threading the plasma sheet (solid gray lines in Fig. 1) are not connected to the IMF, and are therefore 'closed' (*1*, *2*). Topology changes are caused by the process of magnetic

---

‡ This is the author's version of the work. It is posted here by permission of the AAAS for personal use, not for redistribution. The definitive version was published in Science, volume 346 on 19th December 2014, DOI:10.1126/science.1257377.

reconnection, which drives magnetospheric dynamics when the IMF is southward (*1*). Different plasma populations are observed in these regions – plasma in the lobes is very cool, whereas the plasma sheet is more energetic. The key way to distinguish between open and closed magnetic field lines is that electron distributions on closed field lines may exhibit a 'double loss cone', in which the distribution peaks perpendicular to the magnetic field (e.g. *3*). This requires the presence of magnetic mirrors on both sides of the observation site, therefore double loss cones are unambiguous indicators that the magnetic field lines observed by a spacecraft are closed.

A major problem in magnetospheric physics is the adaptation of this picture to times when the IMF is northward. A recent study (*4*) has reported relatively hot plasma in the lobes, which is unexpected in standard magnetosphere model. The authors attributed the presence of the plasma to direct entry of the solar wind, implying that it should be observed on open magnetic field lines. However, similar observations (*5, 6*) have previously been interpreted as spatially separated 'filaments' protruding from the plasma sheet into the lobe (though the authors noted that no theoretical description existed which explained their presence (*6*)). In these studies, the observed plasma has been isotropic, but different magnetic field topologies and interpretations have been inferred due to the absence of evidence of a loss cone.

Another controversy concerns the cause of an auroral configuration called the transpolar arc, which occurs at very high latitudes when the IMF is northward (*7, 8*). There is no consensus on whether transpolar arcs occur on field lines that are closed (*3, 7-10*) or open (*11–13*). Their formation remains the subject of debate, with a range of competing theories (*14–20*). One mechanism for transpolar arcs is for them to result from the closure of lobe magnetic flux which then remains 'trapped' in the magnetotail (*10*); this hypothesis makes a number of predictions that have recently been validated statistically (*14*, *20*). If this is true, a spacecraft situated in the lobe should observe a wedge of closed flux sandwiched within the lobe at high latitudes, well away from the expected location of the plasma sheet.

Virtually all plasma observations of transpolar arcs have come from spacecraft at low altitudes; these observations therefore report the precipitation associated with the arc, rather than a direct measurement of the source plasma for the arc. It has been argued that further examination of in situ observations in the lobes (i.e., at much higher altitudes) is necessary to identify the source plasma and the processes causing transpolar arcs (*8*). To date, only one study has reported such observations (*6*), which revealed relatively hot plasma, similar to the atypically hot lobe plasma signatures discussed above (*4, 5*). The authors concluded that they detected the source plasma for a transpolar arc, but that the observed structures were not explained by any existing theory. Here, we demonstrate that the presence of this plasma can be explained by the 'trapped flux' mechanism for the formation of transpolar arcs (*10*) by showing that a double loss cone is observed within the plasma, and that the plasma observations correspond extremely well to the back-and-forth motion of a transpolar arc.

On 15th September 2005, the Cluster 1 spacecraft was situated in the southern hemisphere lobe (Fig. 1). An overview of the IMF and the observations made by Cluster 1 are shown as a function of time in Fig. 2. The main period of interest is between 16:00 and 19:00 UT, when the IMF was northward ($B_Z > 0$ – Fig. 2a). Before 17:00 and after 19:00 UT, the ions observed were cool (< 500 eV – Fig. 2d), which is consistent with upwelling from the ionosphere and typical of the lobe. However, between 17:00 and 19:00 UT, a much more energetic plasma population was observed (~1 keV electrons and ~10 keV ions – Figs. 2c-d), which is comparable with the mean plasma sheet energy when the IMF is northward (*21*). The electron and ion energies and temperatures (Figs. 2c-e) are comparable with those reported in previous studies (*4*-*6*).

The electron pitch angles observed between 18:15 and 18:45 UT are plotted in Fig. 3a. Cluster 1 observed bidirectional electrons (peaking at pitch angles of 0° and 180°) throughout the interval, except at ~18:36 UT when the electron distribution was not only more intense, but peaked at pitch angles nearer 90°. Figure 3b shows the pitch angle distribution averaged over 21 seconds centered on 18:36:43 UT (indicated as 'G' in Figure 3a). The color scale has been selected to emphasize the variations between different pitch angles. The parallel and antiparallel fluxes were approximately half the value observed perpendicular to the magnetic field. This 'double loss cone' is extremely strong evidence that the plasma observed by Cluster was on closed magnetic field lines. The bidirectional electrons observed beforehand (between 18:15 and 18:35 UT) are also consistent with electrons observed on closed magnetic field lines – in typical magnetotail crossings, bidirectional electrons are observed through much of the outer plasma sheet, with 'double loss cone' distributions deep in the central plasma sheet (*21*). Ion distributions observed at this time are indicative of the occurrence of magnetotail reconnection tailward of the spacecraft (Fig S1).

Simultaneous observations of the southern hemisphere aurora on a global scale are available for this period from the far ultraviolet Wideband Imaging Camera (*22*) on the IMAGE (Imager for Magnetopause-to-Aurora Global Exploration) satellite (Fig. 4a). (The location of IMAGE is also indicated in Fig. 1, and the full sequence of auroral images is shown in Movie S1.) In Fig 4a, the location of Cluster 1 has been mapped onto the southern hemisphere ionosphere along the model magnetic field lines (*23*) of Fig. 2. There is an excellent match between the plasma observations made by Cluster and the location of the transpolar arc relative to the footprint of the spacecraft (see Fig. 2 and Movie S1). The second time that the arc intersects the spacecraft footprint (Fig. 4a, panel G) corresponds with the time that the highest intensities of energetic plasma were observed by Cluster, which is when the double loss cone was observed in Figure 3b.

Our observations demonstrate that atypically hot plasma observed in the lobe occurs on closed magnetic field lines, and is therefore incompatible with direct entry from the solar wind. The excellent match between the plasma observations and the intersections of the transpolar arc and the spacecraft footprints (D, F and G in Figs. 2 and 4) confirms that such atypically hot plasma is the source plasma for transpolar arcs. The correspondence between the intersections of the arc and the observation of hotter plasma at three distinct times also demonstrates that the cause of multiple sequential observations of such atypical plasma is the back-and-forth motion of the closed magnetic field lines – i.e. they are not necessarily spatially-separated filaments as previously proposed (*5*, *6*). Whilst the link with transpolar arcs has previously been suggested (*6*), the confirmation of the magnetic field topology provides strong evidence that both transpolar arcs and atypically hot lobe plasma observed during periods of northward IMF are caused by the process of magnetic reconnection in the magnetotail, where newly-closed lobe flux becomes trapped in the lobe (*10*). Although other proposed mechanisms could explain the closed nature of the magnetic flux threading the transpolar arc, we are not aware of an alternative mechanism that could explain all of the following points: (i) the observation of the lobe immediately before and after the passage of the arc, (ii) the observed back-and-forth motion of the arc, and (iii) the absence of a change in sign of the IMF B_Y component in the hour before the arc formed (see supplementary online text). The reconnection mechanism (*10*) predicts that closed magnetic flux observed at high latitudes should be similar in most respects to the plasma sheet, because both contain plasma that was originally contained in the lobe but that has since been heated as a result of the contraction of the field lines following their closure. Our observations confirm that the plasma observed at high latitudes is indeed similar to that observed in the plasma sheet. The net effect of this process is an increase in the closed fraction of the magnetotail in one narrow local time sector. An interesting consequence is that as this transpolar arc spans the entire polar cap, the magnetotail is entirely closed in a narrow sector of local time, which highlights the intriguing topology that the magnetosphere can attain when the IMF points northward.

References and Notes:

1. J. W. Dungey, *Phys. Rev. Lett.* **6**, 47 (1961).
2. J. W. Dungey, in *Geophysics: The Earth's Environment*, C. DeWitt, J. Hieblot, A. Lebeau, eds. (Gordon and Breach, New York, 1963), pp. 505–550.
3. J. D. Menietti, J. L. Burch, *J. Geophys. Res.* **92**, 7503 (1987).
4. Q. Q. Shi, *et al.*, *Nat. Commun.* **4**, 1466 (2013).
5. C. Y. Huang, *et al.*, *J. Geophys. Res.* **92**, 2349 (1987).
6. C. Y. Huang, J. D. Craven, L. A. Frank, *J. Geophys. Res.* **94**, 10137 (1989).
7. L. A. Frank, J. D. Craven, J. L. Burch, J. D. Winningham, *Geophys. Res. Lett.* **9**, 1001 (1982).
8. L. A. Frank, *et al.*, *J. Geophys. Res.* **91**, 3177 (1986).
9. W. K. Peterson, E. G. Shelley, *J. Geophys. Res.* **89**, 6729 (1984).
10. S. E. Milan, B. Hubert, A. Grocott, *J. Geophys. Res.* **110**, A01212 (2005).
11. D. A. Hardy, W. J. Burke, M. S. Gussenhoven, *J. Geophys. Res.* **87**, 2413 (1982).
12. M. S. Gussenhoven, E. G. Mullen, *J. Geophys. Res.* **94**, 17121 (1989).
13. N. Østgaard, S. B. Mende, H. U. Frey, L. A. Frank, J. B. Sigwarth, *Geophys. Res. Lett.* **30**, 2125 (2003).
14. R. C. Fear, S. E. Milan, *J. Geophys. Res.* **117**, A03213 (2012).
15. A. Kullen, M. Brittnacher, J. A. Cumnock, L. G. Blomberg, *J. Geophys. Res.* **107**, 1326 (2002).
16. N. Østgaard, *et al.*, *J. Atmos. Sol.-Terr. Phy.* **69**, 249 (2007).
17. A. Goudarzi, M. Lester, S. E. Milan, H. U. Frey, *Ann. Geophys.* **26**, 201 (2008).
18. J. A. Cumnock, *et al.*, *J. Geophys. Res.* **116**, A02218 (2011).
19. A. Kullen, in *Auroral Phenomenology and Magnetospheric Processes: Earth and Other Planets*, A. Keiling, E. Donovan, F. Bagenal, T. Karlsson, eds., Geophysical Monograph 197 (American Geophysical Union, Washington D. C., 2012), pp. 69–80.
20. R. C. Fear, S. E. Milan, *J. Geophys. Res.* **117**, A09230 (2012).
21. A. P. Walsh, *et al.*, *J. Geophys. Res.* **118**, 6042 (2013).

22. S. B. Mende, *et al.*, *Space Sci. Rev.* **91**, 271 (2000).

23. N. A. Tsyganenko, *Proc. Third International Conference on Substorms (ICS-3)* (ESA SP-389, 1996), pp. 181–185.

24. C. T. Russell, *Cosmic Electrodyn.* **2**, 184 (1971).

25. J. H. King. N. E. Papitashvili, *J. Geophys. Res.*, **110**, A02104 (2005).

26. A. N. Fazakerley, *et al.*, in *The Cluster Active Archive - Studying the Earth's Space Plasma Environment*, H. Laakso, M. Taylor, P. Escoubet, eds. (Springer Netherlands, Dordrecht, 2010), pp. 129–144.

27. H. Rème, *et al.*, *Ann. Geophys.* **19**, 1303 (2001).

28. Y. T. Chiu, N. U. Crooker, D. J. Gorney, *J. Geophys. Res.* **90**, 5153 (1985).

29. L. R. Lyons, *J. Geophys. Res.* **90**, 1561 (1985).

30. J. J. Sojka, L. Zhu, D. J. Crain, R. W. Schunk, *J. Geophys. Res.* **99**, 8851 (1994).

31. H. C. Carlson, S. W. H. Cowley, *J. Geophys. Res.* **110**, A05302 (2005).

32. K. Makita, C.-I. Meng, S.-I. Akasofu, *J. Geophys. Res.* **96**, 14085 (1991).

33. A. Kullen, *Geophys. Res. Lett.* **27**, 73 (2000).

34. S. W. H. Cowley, *Planet. Space Sci.* **29**, 79 (1981).

35. A. Kullen, P. Janhunen, *Ann. Geophys.* **22**, 951–970 (2004).

36. S. M. Naehr, F. R. Toffoletto, *J. Geophys. Res.* **109**, A07202 (2004).

37. T. Tanaka, T. Obara, M. Kunitake, *J. Geophys. Res.* **109**, A09201 (2004).

38. M. Watanabe, G. J. Sofko, *J. Geophys. Res.* **113**, A09218 (2008).

Acknowledgments: Work in the UK was supported by STFC Ernest Rutherford Fellowship ST/K004298/1 and STFC grants ST/K001000/1 and ST/K000977/1. RM is supported by the Belgian Science Policy Office through the Solar-Terrestrial Center of Excellence. French participation in the Cluster project is funded by CNES. IMAGE satellite work at the University of California, Berkeley was supported through a SWRI subcontract under NASA contract NAS5-96020. We acknowledge support from the International Space Science Institute through funding of their International Team on Polar Cap Arcs, and we are grateful for discussions with members of the team. Cluster data were obtained from the Cluster Active Archive (http://caa.estec.esa.int/caa/), and the IMAGE FUV data were provided by the NASA Space Science Data Center (http://nssdc.gsfc.nasa.gov/space/). The OMNI IMF data were obtained through the NASA's CDAWeb (http://cdaweb.gsfc.nasa.gov/), for which we acknowledge J. H. King, N. Papatashvilli and the PIs of the magnetic field and plasma instruments on the Geotail and ACE spacecraft. The DMSP particle detectors were designed by Dave Hardy of AFRL, and data obtained from JHU/APL.

Fig. 1. The locations of the Cluster 1 and IMAGE spacecraft between 17:00 UT (indicated by asterisks) and 19:00 UT on 15th September 2005. Positions are projected into the XZ plane of the Geocentric Solar Magnetic coordinate system (*24*), in which the X axis is directed towards the Sun and Z is towards magnetic north. Solid black lines indicate model locations for the bow shock and magnetopause; gray lines indicate model geomagnetic field lines from an empirical model (*23*). The field lines which are expected to be 'closed' are plotted as solid lines, whilst those which would normally be 'open' and hence connected to the solar wind downtail are dashed. Cluster 1 was deep inside the lobe, a long way from the expected location of the closed field line region (the plasma sheet).

Fig. 2. Time series of the interplanetary and magnetospheric conditions. The top two panels show the simultaneous (a) north/south and (b) east/west components of the IMF (B_Z and B_Y respectively) obtained from the OMNI dataset (*25*). The next two panels show the (c) electron and (d) ion populations observed by Cluster 1 in the magnetotail lobes by the PEACE (*26*) and CIS-HIA (*27*) instruments respectively. Both panels contain the differential energy flux of the electron or ion population plotted as a function of energy and time. The bottom panel (e) shows the observed ion temperature. Arrows labeled with capital letters (A) to (I) indicate selected times of interest.

Fig. 3. (a) The pitch angle distribution of electrons observed above 100 eV between 18:15 and 18:45 UT. (b) The electron distribution observed at the time of the highest differential energy fluxes observed by Cluster (corresponding to arrow (G) in Figure 2, also indicated in Figure 3a). The distribution has been computed from five consecutive spacecraft spin periods, centered on time G, and the color scale has been chosen to emphasize the differences in the field-aligned and perpendicular directions.

Fig. 4. (a) A montage of the auroral observations made by the IMAGE FUV Wideband Imaging Camera on 15th September 2005. Each image has been projected onto a grid of magnetic latitude against magnetic local time with local noon at the top and dawn to the right. Panels (A) to (J) show the transpolar arc (indicated by the white arrow in (B)) at different stages of its evolution, with the footprint of the Cluster spacecraft indicated by a red dot. The times corresponding to Panels (A) to (J) are also indicated in Fig. 2 and Fig. 4b. At 15:10 UT (A), the aurora conformed to the standard 'oval' configuration, and the Cluster 1 footprint was in the dim region poleward of the main auroral oval (the polar cap), consistent with the location of the spacecraft in the lobe. At 16:38 UT (B), a small feature emerged from the nightside oval (indicated by the white arrow) which subsequently grew into a transpolar arc (C-I). The growth and evolution of the arc (B-H) occurred whilst the IMF was northward (Figure 2a). The arc was initially duskward of the footprint of Cluster (B-C). At 17:16 UT (D) the arc intersected the spacecraft footprint before retreating duskward again (E); a subsequent and final period of dawnward motion caused the arc to intersect the spacecraft footprint once more (F-G) and then move past the spacecraft footprint (H-I). After the IMF turned southward at 19:10 UT, the arc

retreated to the night side of the polar cap (I), and subsequently disappeared (J). (b) The electron population observed by Cluster (replotted from Figure 2c), with labels showing the times corresponding to (A)-(I). There is an excellent correspondence between the times that the uncharacteristic plasma is observed and the times where the transpolar arc intersected the spacecraft footprint (D, F and G). (c) Spectrograms of the electron and ion populations observed by the DMSP F16 satellite at low altitude during a polar cap crossing made between (F) and (G). Ion precipitation was observed between 18:25 and 18:27 UT, which coincides with the time that the DMSP (Defense Meteorological Satellite Program) F16 satellite traversed the arc. (The orbit of the DMSP spacecraft is shown in Figure 4a in panel (F).) The ion and electron precipitation observed at this time is comparable in energy with that observed above the main oval (*7*, *9*) and at high altitudes by Cluster 1 (Figure 2c-d), although the electron precipitation observed by DMSP shows signs of further acceleration (inverted 'V's). In these respects, the precipitation observed by DMSP is typical for transpolar arcs (e.g. *18*). Electron precipitation is observed elsewhere in the polar cap, and may be associated with fainter polar cap arcs, presumably on open magnetic field lines.

Supplementary Materials:

Supplementary online text

Figure S1

Movie S1

References (*28*-*38*)

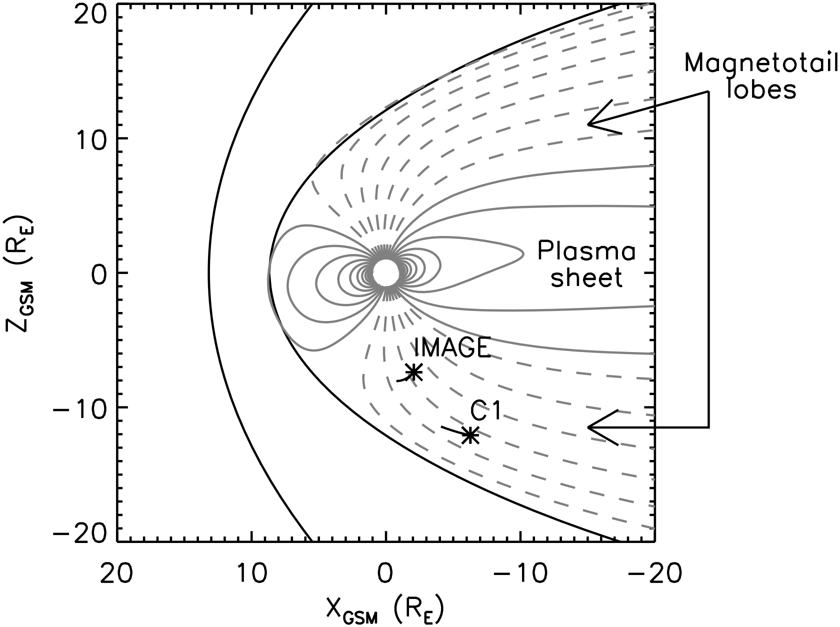

Magnetotail
lobes
Plasma
sheet
IMAGE
C1
20
10
0
−10
−20
Z_{GSM} (R_E)
X_{GSM} (R_E)

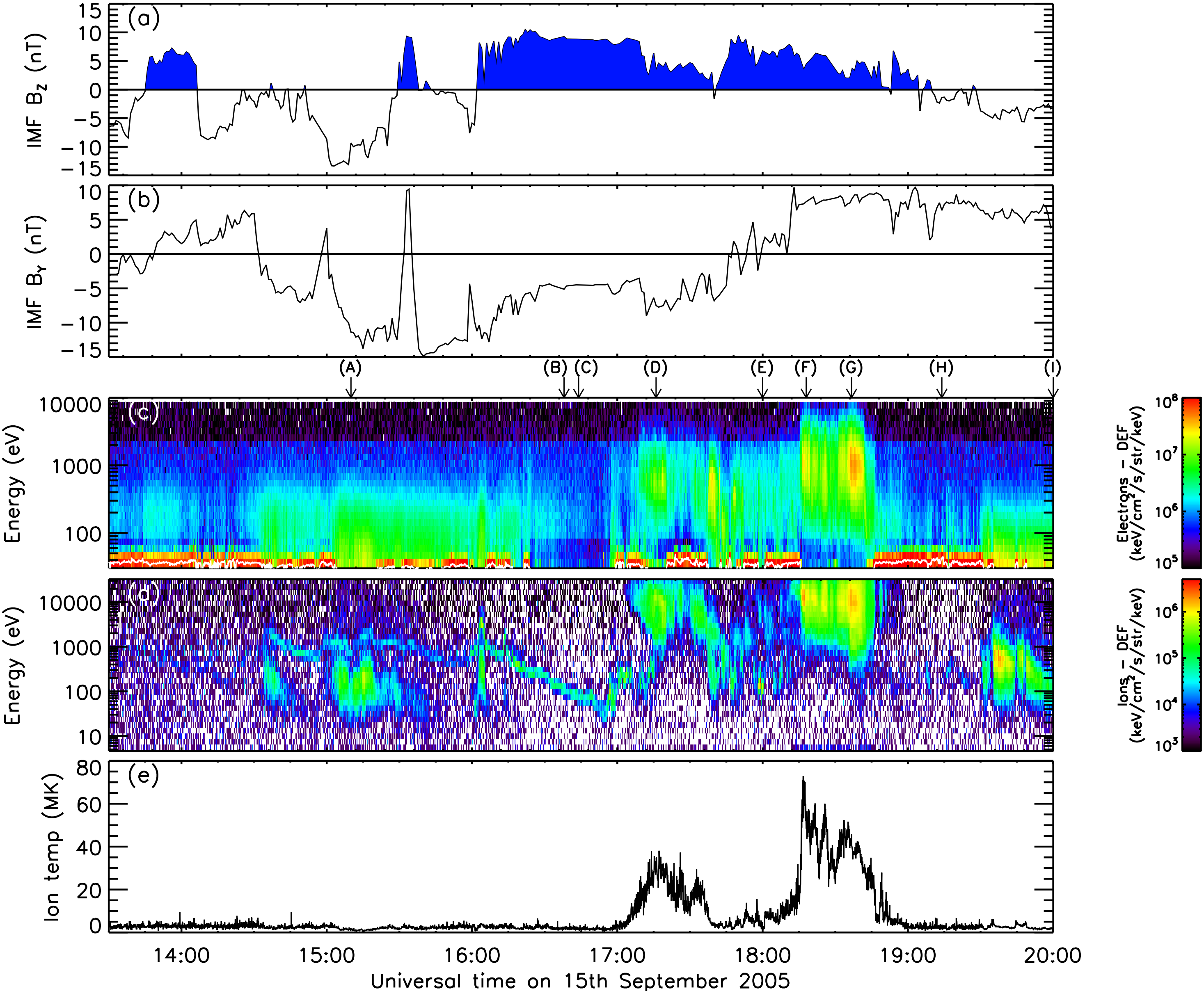

(a)
IMF B_Z (nT)
15
10
5
0
−5
−10
−15
(b)
IMF B_Y (nT)
10
5
0
−5
−10
−15
(A)
(B)
(C)
(D)
(E)
(F)
(G)
(H)
(I)
(c)
Energy (eV)
10000
1000
100
Electrons – DEF (keV/cm²/s/str/keV)
10⁸
10⁷
10⁶
10⁵
(d)
Energy (eV)
10000
1000
100
10
Ions – DEF (keV/cm²/s/str/keV)
10⁶
10⁵
10⁴
10³
(e)
Ion temp (MK)
80
60
40
20
0
14:00
15:00
16:00
17:00
18:00
19:00
20:00
Universal time on 15th September 2005

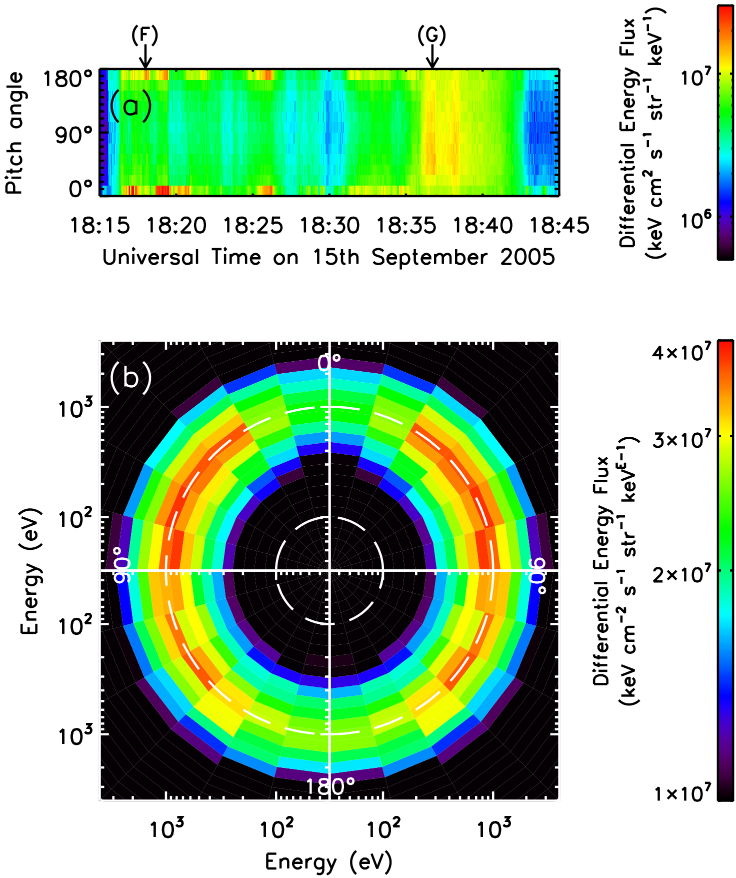
(F)
(G)
(a)
Pitch angle
180°
90°
0°
18:15 18:20 18:25 18:30 18:35 18:40 18:45
Universal Time on 15th September 2005
Differential Energy Flux
(keV cm^2 s^{-1} str^{-1} keV^{-1})
10^7
10^6
(b)
0°
90°
90°
180°
Energy (eV)
10^3
10^2
10^2
10^3
10^3 10^2 10^2 10^3
Energy (eV)
Differential Energy Flux
(keV cm^{-2} s^{-1} str^{-1} keV^{E-1})
4×10^7
3×10^7
2×10^7
1×10^7

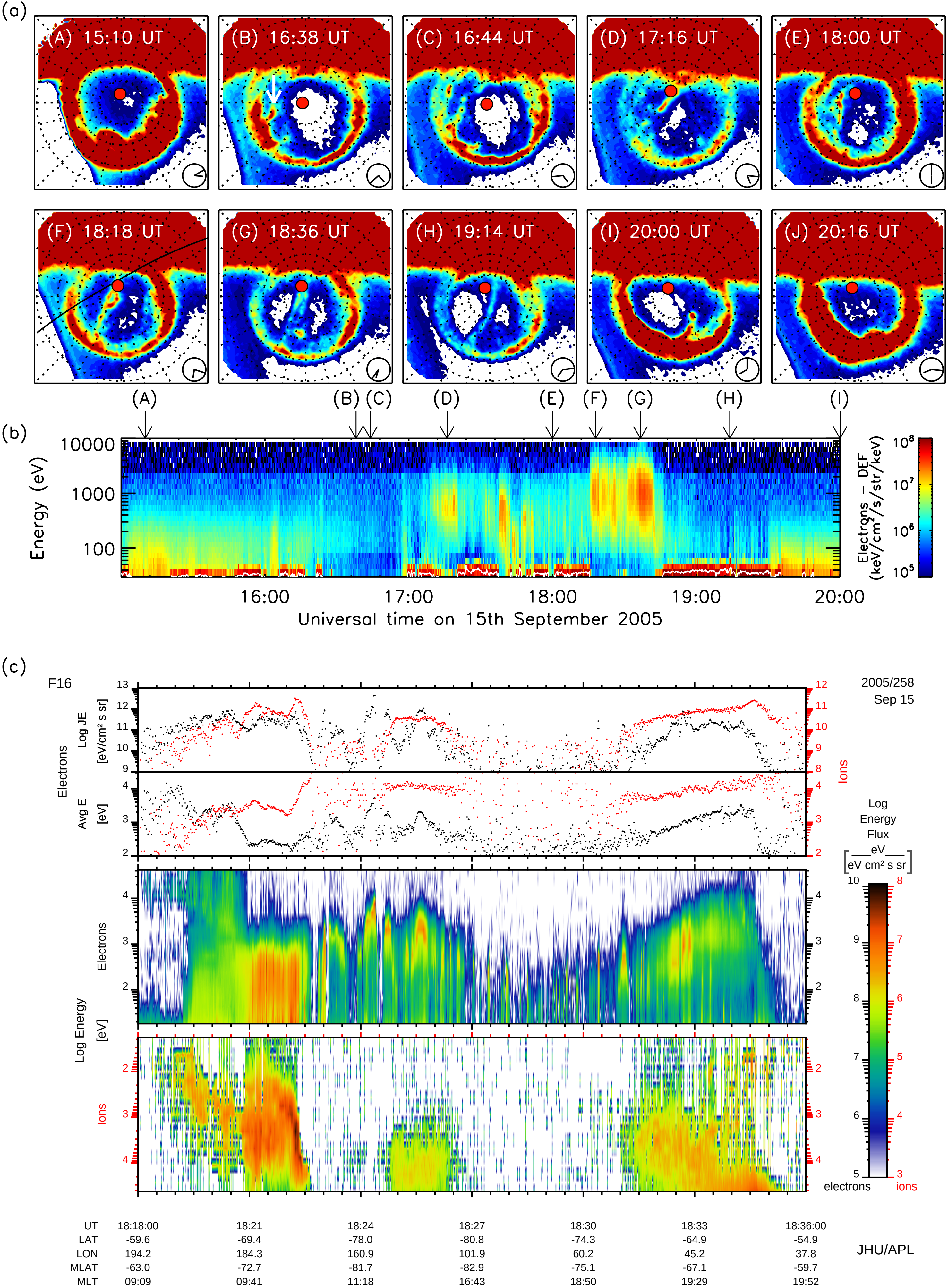
(a)
(A) 15:10 UT
(B) 16:38 UT
(C) 16:44 UT
(D) 17:16 UT
(E) 18:00 UT
(F) 18:18 UT
(G) 18:36 UT
(H) 19:14 UT
(I) 20:00 UT
(J) 20:16 UT
(A) (B) (C) (D) (E) (F) (G) (H) (I)
(b)
Energy (eV)
10000
1000
100
16:00 17:00 18:00 19:00 20:00
Universal time on 15th September 2005
Electrons – DEF (keV/cm2/s/str/keV)
10^8 10^7 10^6 10^5
(c)
F16
2005/258
Sep 15
Electrons
Log JE [eV/cm² s sr]
Avg E [eV]
Ions
Log Energy Flux [eV / eV cm² s sr]
Electrons
Log Energy [eV]
Ions
electrons
ions
UT 18:18:00 18:21 18:24 18:27 18:30 18:33 18:36:00
LAT -59.6 -69.4 -78.0 -80.8 -74.3 -64.9 -54.9
LON 194.2 184.3 160.9 101.9 60.2 45.2 37.8
MLAT -63.0 -72.7 -81.7 -82.9 -75.1 -67.1 -59.7
MLT 09:09 09:41 11:18 16:43 18:50 19:29 19:52
JHU/APL

Science AAAS

Supplementary Materials for

Direct observation of closed magnetic flux trapped in the high latitude magnetosphere

R. C. Fear, S. E. Milan, R. Maggiolo, A. N. Fazakerley, I. Dandouras, S. B. Mende.

Correspondence to: R.C.Fear@soton.ac.uk

This PDF file includes:

Supplementary Text
Fig. S1
Caption for Movie S1

Other Supplementary Materials for this manuscript includes the following:

Movie S1

Supplementary Text

Constraints on formation mechanisms

The observations reported in this paper present several constraints on mechanisms proposed for the formation of transpolar arcs.

The fact that the plasma observed is on closed magnetic field lines rules out those mechanisms in which transpolar arcs are the consequence of field aligned currents directly driven by velocity shears caused by convection of plasma in the lobe (*28–30*), although these mechanisms might still explain other, fainter, polar cap auroras (*31*).

The observation of typical lobe plasma immediately before and after the atypical plasma distributions (at labels (C) and (H) in Figure 2) indicate that the transpolar arc is sandwiched between regions of lobe magnetic flux. This rules out mechanisms which propose that the transpolar arc is in fact part of the main auroral oval (*32*).

The two changes in direction of motion of the arc (which result in two separate periods of observation of the atypical lobe plasmas) are fully consistent with the hypothesis that the closed magnetic flux that threads the transpolar arc (and which is observed by Cluster) moves with the lobe convection pattern (*10*). The first period of dawnward motion (Figure 4a, panels B-D) corresponds to a period when the IMF B_Y component is negative (Figure 2b); during this period, we would expect the polar cap convection pattern to be dominated in the southern hemisphere by the dawn cell, but the transpolar arc, situated on the dusk side of the polar cap, to be located on the dusk cell and hence move dawnward (*10*). The first change in motion (Figure 4a, panels D-E) corresponds to an increase in the magnitude of the (negative) IMF B_Y component. This should cause an expansion of the dawn convection cell, which would explain the duskward motion of the arc (*10*). Finally, the second period of dawnward motion (Figure 4a, panels E-J) starts when the IMF B_Y component changes sign. The resulting period of dawnward motion is fully consistent with a dominant dusk cell.

This complex motion cannot be explained by mechanisms which describe the arc as the consequence of the tailward propagation of a ‘twist’ in the magnetotail, resulting in more complex mapping of the distant plasma sheet to the ionosphere such that the distant plasma sheet maps to poleward of the auroral oval (*33*). Such interpretations predict that an arc will form at one side of the auroral oval and move dawnward or duskward (depending on the sense of the B_Y sign change) to the other. Each rotation in the IMF may introduce a fresh twist into the magnetotail (*34*), but once a new twist has been introduced it must propagate downtail and therefore the arc will continue to move in the same direction. Consequently, such mechanisms cannot explain a change in direction of the arc as observed in Figure 4a (panels D-F), or the multiple observations of hot lobe plasma in Figure 2.

Several MHD simulations have simulated the effect of changing IMF B_Y during intervals when the IMF is northward (*35*-*37*); the interpretation has generally been that the transpolar arc is formed as a direct result of the change in the direction in which the magnetotail twists, as a result of a new IMF B_Y direction (*35*-*37*). In this manner, the interpretation is similar to the conceptual model based on tailward propagation of a magnetotail twist (*33*), although it has also been suggested that magnetotail reconnection may instead be playing a role in the formation of the transpolar arc in these simulations (*38*). Either way, a change in the sign of the IMF B_Y component is required to trigger the arc in these simulations; none of the interpretations proposed in these papers (*35*-*38*) allow the occurrence of a transpolar arc if the IMF B_Y component is steady beforehand. This is incompatible with the present set of observations, as the IMF B_Y component was steadily negative for an hour before the transpolar arc was first observed (prior to label '(B)' in Figure 2). Furthermore, in these simulations the introduction of a second change in the IMF B_Y direction results in the addition of a second transpolar arc (*36*); it does not change the direction of motion of the original arc as observed in the present event. Whilst the alternative explanation (*38*) of the simulation runs shares some interesting similarities with the reconnection-based model discussed in the main body of the paper (*10*), it differs in that it also requires a change in the sign of IMF B_Y to trigger the formation of the transpolar arc, which is not observed in this event.

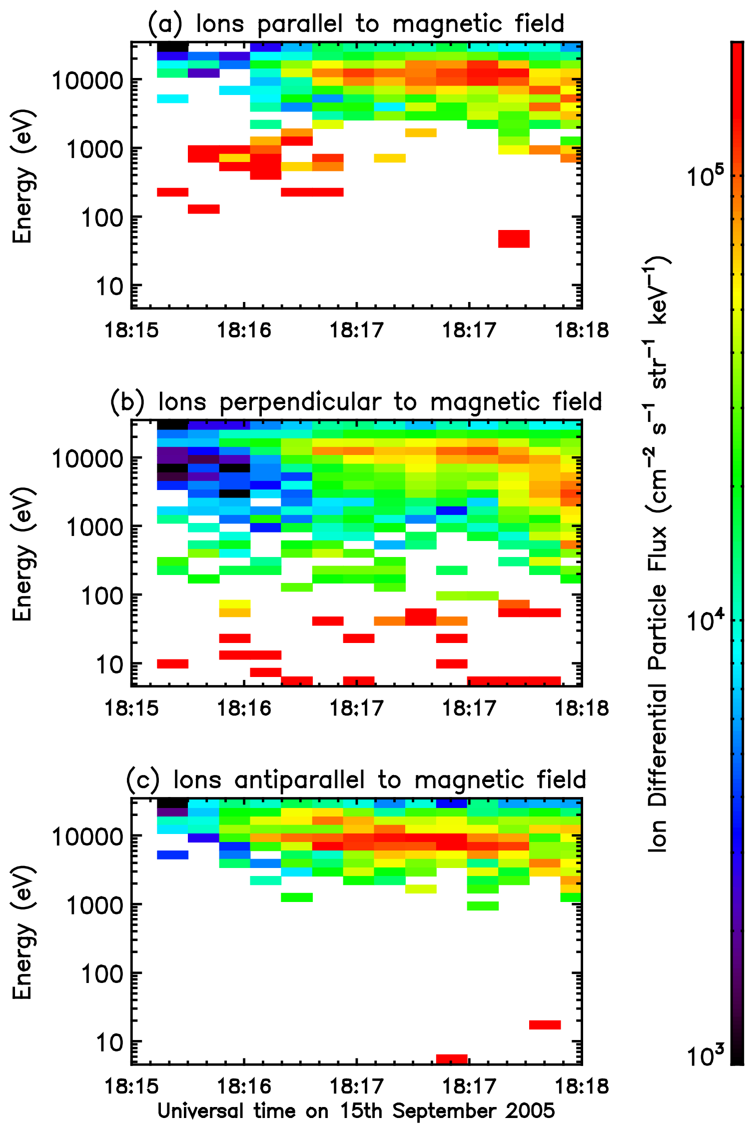

Fig. S1.

The ion energy distributions observed (a) parallel, (b) perpendicular and (c) antiparallel to the magnetic field at the time the energetic plasma was first observed (18:15 to 18:18 UT), which is near the time labelled (F) in Figs 2-4. Between 18:16 and 18:17 UT, the energetic ions above 10 keV were observed predominantly antiparallel to the magnetic field (i.e. moving Earthward – Figure S1c), which is indicative of the occurrence of magnetotail reconnection tailward of the spacecraft.

Movie S1

A summary of the correspondence of the auroral and plasma observations. (a) The auroral observations summarized in Figure 4. (b) The location of Cluster 1 at the time corresponding to the image in (a), in a similar format to Figure 1. (c)-(f) The interplanetary magnetic field and magnetotail electron/ion spectrograms (same format as Figure 2a-d); the time corresponding to panels (a) and (b) of this movie is indicated with a red vertical line.